Single-Particle and Collective Dynamics of Protein Hydration Water: A Molecular Dynamics Study

M. Tarek[1,2,*] and D. J. Tobias[3]

[1]*NIST Center for Neutron Research, National Institute of Standards and Technology, Gaithersburg, Maryland 20899-8562*
[2]*Chemistry Department, University of Pennsylvania, Philadelphia, Pennsylvania 19103-6323*
[3]*Department of Chemistry, University of California, Irvine, California 92697-2025*
(Received 11 June 2002; published 17 December 2002)

We present an analysis based on molecular dynamics simulations of water single particle and collective density fluctuations in a protein crystal at 150 and 300 K. For the collective dynamics, the calculations predict the existence of two sound modes. The first one around 35 meV is highly dispersive and the second one around 9 meV is weakly dispersive in the k range studied here ($0.5 < k < 4.2$ Å^{-1}). We provide evidence that the boson peak around 4 meV in the single particle spectra arises from translational motion, is present in the coherent spectra, and is distinct from the two sound modes.

DOI: 10.1103/PhysRevLett.89.275501 PACS numbers: 61.20.Ja, 64.70.Pf, 87.14.Ee, 87.15.Aa

Protein hydration water is important for protein structure and stability, and influences the dynamics of the protein molecule as a whole [1]. Numerous experimental and theoretical studies have demonstrated that dynamical properties of hydration water are different from those of bulk water. Single particle motion studied by NMR relaxation techniques [2] and intermolecular spin relaxation [3] show that, due to hydrogen bonding to the protein external side chains, water rotation and translation are slowed down on the surface of the protein. The anomalous behavior of water at the protein surface has also been a subject of investigation by both inelastic neutron scattering [4] and molecular dynamics (MD) simulations [5–7]. Hydration water displays dynamical characteristics that can be described in terms of an α relaxation model used for dense supercooled liquids [4]. Furthermore, it has been shown that the single particle dynamical spectra present a low frequency vibrational anomaly (the boson peak) typical of glassy materials [5]. Because of experimental limitations, nothing is known about the collective dynamics of protein hydration water. However, with recent progress in inelastic x-ray techniques it may soon be possible to investigate coherent density fluctuations in protein systems. Here we characterize collective density fluctuations in protein hydration water using MD simulations, and predict that they exhibit two sound modes that are similar to those observed previously in liquid water [8–13], as well as intensity in the boson peak range that is absent in liquid water. We also present an analysis of the single particle motion in order to clarify the origin of the boson peak. By comparing single particle and collective dynamics, we demonstrate that boson peak excitations are distinct from sound modes over the momentum transfer range accessible in the simulations.

The results presented here are obtained from MD simulations of ribonuclease A (RNase) crystals at 300 and 150 K, and a hydration level of about 0.5 g H_2O/g protein. The snapshot in Fig. 1 depicts the water distribution in the crystal. Details about the simulation protocols were reported previously [6,7]. We have used the CHARMM22 [14] force field for the protein, the SPC/E model for water [15], and have demonstrated that the crystal structure over a wide range of temperatures (100 to 300 K) is well reproduced [7]. We have shown that the water dynamical properties in the crystal are identical to those in powder environments (used in neutron experiments) at similar hydration levels [6,7]. Extensive comparison to inelastic neutron experiments confirmed that the water single particle motion can be quantitatively reproduced by MD simulation [7]. The calculations were carried at constant temperature and pressure [16]. A multiple time step algorithm [17] was used to integrate the equations of motions with a time step of 4 fs. MD trajectories of ≈ 1 ns duration were generated for each system, and the last 100 ps of each run was used for analysis. Although water dynamical processes on the

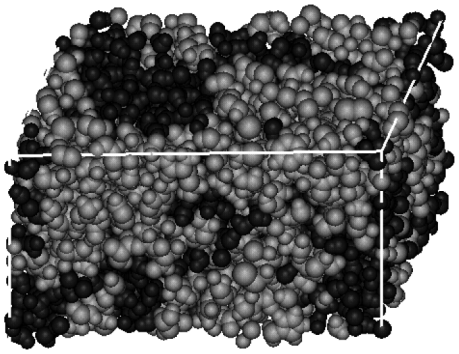

FIG. 1. Snapshot from a MD simulation of the RNase crystal. The simulation box corresponds to one crystal unit cell containing 2 protein molecules (light atoms) and 817 water molecules (dark atoms). The box is replicated infinitely in three dimensions using periodic boundary conditions.

surface of a protein span a wide range of time scales [2–4], the density fluctuations of interest here occur on the ps time scale, and hence are sampled well during our analysis period.

The dynamics of collective density fluctuations is determined experimentally by measuring the coherent dynamical structure factor $S_c(k, E)$, the space and time Fourier transform of the particle density pair correlation function at a wave vector k and energy E. The single particle motion is described by $S_s(k, E)$, the self part of the dynamical structure factor. $S_c(k, E)$ and $S_s(k, E)$ are the time Fourier transforms (FT) of the coherent and incoherent intermediate scattering functions, $I_c(k, t) = \langle \sum_{\alpha\beta} f_\alpha^c(k) f_\beta^c(k) \exp\{\imath \mathbf{k} \cdot [\mathbf{r}_\alpha(t) - \mathbf{r}_\beta(0)]\} \rangle / N$ and $I_s(k, t) = \langle \sum_\alpha f_\alpha^i(k) f_\alpha^i(k) \exp\{\imath \mathbf{k} \cdot [\mathbf{r}_\alpha(t) - \mathbf{r}_\alpha(0)]\} \rangle / \mathrm{N}$, respectively, where $\mathbf{k}$ is the momentum transfer, $\mathbf{r}_\alpha(t)$ is the position of the αth scatterer at time t, $f_\alpha^{c/i}(k)$ is its form factor, N the number of scatterers, and the angular brackets denote an average over time origins. Both intermediate scattering functions can be calculated directly from MD trajectories, and the corresponding spectra compared to inelastic neutron and x-ray experiments, which probe the incoherent and coherent contributions, respectively. In practice a time window corresponding to a particular instrumental resolution is used to avoid truncation artifacts in the FT. The spectra reported here were computed with an energy resolution of 1.5 meV, which is characteristic of current inelastic x-ray spectrometers [18], and corresponds to a time scale of ≈ 1 ps.

Access to the water dynamics from such experiments is not trivial. In neutron experiments, the incoherent scattering amplitude is mainly contributed by hydrogen atoms. One therefore has to deuterate the protein in order to minimize its scattering, or subtract spectra obtained for hydrogenated proteins in H_2O and D_2O. In x-ray experiments, the scattering amplitude is proportional to the atomic form factor, $f_\alpha(k)$, a k-dependent quantity whose magnitude is equal to the atomic number Z of the atom at $k = 0$. For the protein/water system, the coherent scattering is contributed by all heavy atoms. Separation of protein and water contributions can be achieved only by modeling the data. MD simulation results may be used to generate the total scattering for direct comparison with neutron and x-ray data. To probe water dynamics specifically, it is possible to isolate water scattering by simply ignoring contributions to the dynamical structure factor from the protein atoms.

Figure 2(a) reports the coherent dynamical structure factor $S_c(k, E)$ for water generated from the simulation of the RNase crystal at 150 K for selected wave vectors k [19]. The spectra show a peak around 4–5 meV. The presence of higher frequency peaks in the structure factor is revealed in the longitudinal current spectra, $C_L(k, E) = (E^2/k^2) S_c(k, E)$, displayed in Fig. 2(b). The $C_L(k, E)$ display two peaks, whose intensity depends on k. The first is located around 10 meV, and the second between 15 and 40 meV, depending on the k value.

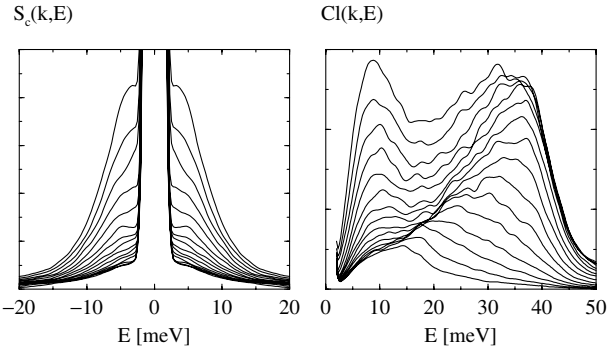

FIG. 2. Coherent dynamical structure factors $S_c(k, E)$ and corresponding longitudinal spectra $C_L(k, E)$ for the protein hydration water in simulations of the RNase crystal at 150 K for selected values of the momentum transfer ($k = 0.5$ to 1.9 Å^{-1}, increasing from bottom to top at intervals of 0.1 Å^{-1}).

Contour plots of the longitudinal spectra at k values ranging from 0.5 to 4 Å^{-1} are displayed in Fig. 3. At low k the high frequency Brillouin side peak is clearly dispersive with k at both 150 and 300 K. The low frequency peak has a nearly constant frequency (≈ 10 meV) in the k range studied here. These results are very similar to those reported for liquid water [20]. Indeed, inelastic neutron scattering and x-ray experiments have revealed the existence of two Brillouin modes [9–13] as predicted by the pioneering simulations of Rahman and Stillinger [8]. At 278 K these modes, commonly referred to as "ordinary" and "fast" sound, propagate at 1500 m · s^{-1} and 3200 m · s^{-1}, respectively [8,20]. More recently, it has been shown for liquid water, by analysis of both the transverse and longitudinal current spectra [21], that the low energy peak, which is not dispersive at $k > 0.7$ Å^{-1}, arises from the transverse dynamics (propagating with sound speed 1500 m · s^{-1}), while the high frequency peak is the ordinary sound (propagating at 1500 m · s^{-1} at low k and 3200 m · s^{-1} at high k). In the present study, we are limited to $k > 0.5$ Å^{-1} [19], so we only have access to the fast sound speed through the slope of the maximum of the higher frequency peak as a function of k

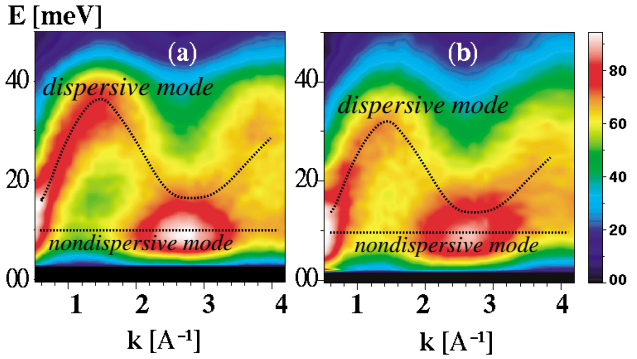

FIG. 3 (color). Contour plots of the longitudinal current spectra $C_L(k, E)$ for the protein hydration water from the simulations of the RNase crystal at 150 K (a) and 300 K (b).

at small k. The values extracted from our data are 4500 $m \cdot s^{-1}$ at 100 K and 3800 $m \cdot s^{-1}$ at 300 K.

The incoherent dynamical structure factors, $S_s(k, E)$, calculated for the water protons in the RNase crystal are reported in Fig. 4(a). These results are in excellent agreement with neutron data reported recently for hydrated plastocyanin powders [5]. At 150 K, the spectrum shows a ''boson peak'' at around 3–4 meV. As the temperature is increased to 300 K, the peak either disappears or is buried in the quasielastic signal.

The boson peak has been ascribed to vibrations because it also appears as an excess over the Debye level in the vibrational density of states [5]. The low frequency boson peak ''vibrations'' could have translational and/or rotational character. Decompositions of $I_s(k, t)$ and $S_s(k, E)$ into rotational and translational contributions [7] are displayed in Figs. 4(b) and 4(c). Only the translational component (associated with the motion of the oxygen atoms) contributes to the low frequency peak. In the corresponding dynamical susceptibility spectra (Fig. 4(d)), $\chi''(k, E) = [E/(2k_BT)]S(k, E)$, we recover the well-known TA_1 peak around 6–7 meV, and the librational peak above 40 meV, in agreement with experimental data on myoglobin hydration water [4] and liquid water [22]. At first glance it may seem that the scaling with E shifts the 3 meV boson peak in $S(k, E)$ such that it appears between 6 and 7 meV in the susceptibility spectra. However, as we will demonstrate below, this is not the case. Rather, the boson peak is manifested as a shoulder in the low frequency part of the TA_1 translational peak in $\chi''(k, E)$.

In order to investigate the interplay between the low frequency sound mode and the boson peak we have carried out a series of simulations aimed at perturbing the water dynamics, while monitoring the water dynamical structure factors. Because of the apparent connection between the boson peak of the protein and that of the water [5], we expect that perturbing the dynamics of the protein molecules will have a profound effect on the water dynamics. We have shown in a previous study that the boson peak of the protein reflects the motion of both the backbone and the side chains [23]. It is therefore possible to affect the low frequency spectra of the protein by fixing carbon atoms belonging to the backbone. While this procedure is artificial, the main goal is to perturb the water dynamics. A series of trajectories has been generated at 150 K for four systems in which an increasing number of C^α atoms along the protein backbone have been fixed in space during the simulation. We refer to these systems as follows: (1) no constraints; (2) lysine C^α (total 10) fixed; (3) lysine, alanine, cysteine, and threonine C^α (total 45) fixed; (4) all carbon C^α (total 124) fixed. For each system, an equilibration run of 100 ps was performed, followed by a 40 ps run that was used for the analysis.

The incoherent scattering functions computed from the simulations of systems 1 to 4 are displayed in Fig. 5, along with the corresponding susceptibility spectra. In Fig. 5(a), we see that the boson peak intensity decreases dramatically as the number of fixed protein C^α atoms is increased. We have also included the spectra from a simulation where *all* the protein atoms were held fixed. In this case, where the water molecules are moving in a fixed matrix formed by the surrounding protein molecules, the water boson peak at ≈ 3 meV has completely vanished. The susceptibility spectra enable us to simultaneously follow both the familiar TA_1 peak and the boson peak as the constraints are imposed. Figure 5(b) clearly demonstrates that the boson peak appears as a shoulder on the low frequency side of the TA_1 peak.

Figure 6 displays the coherent structure factors of the unconstrained system, and the system where all the protein atoms were held fixed, at selected k values. As in the incoherent spectra, the intensity in the boson peak region (≈ 3 meV) has drastically decreased in the system with the protein fixed. The corresponding longitudinal spectra

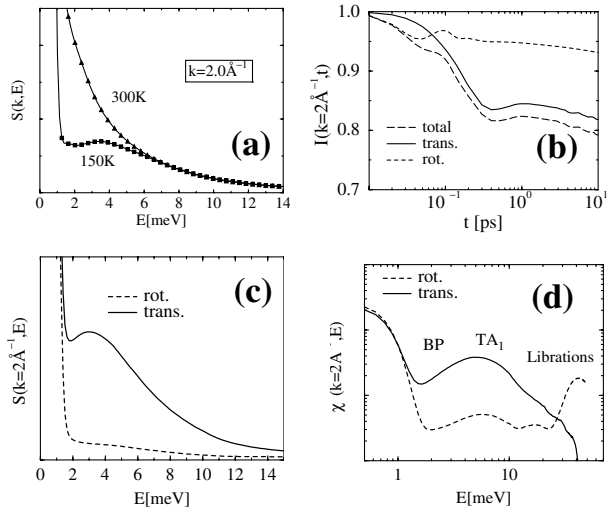

FIG. 4. Hydration water single particle dynamics in the RNase crystal. (a) Water protons $S_s(k, E)$ at 300 and 150 K. (b) Decomposition of the water proton $I_s(k, t)$ into rotational and translational contributions; (c) the corresponding $S_s(k, E)$ and (d) dynamical susceptibility spectra $\chi''(k, E)$ at 150 K.

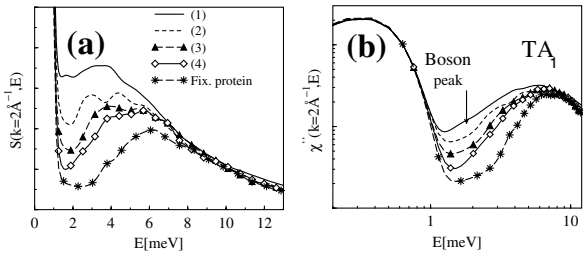

FIG. 5. (a) Water incoherent structure factors $S_s(k, E)$ and (b) dynamical susceptibilities $\chi''(k, E)$ from the simulations at 150 K of systems 1 to 4 where increasing numbers of protein backbone atoms were held fixed, and the results from the system in which all the protein atoms were held fixed.

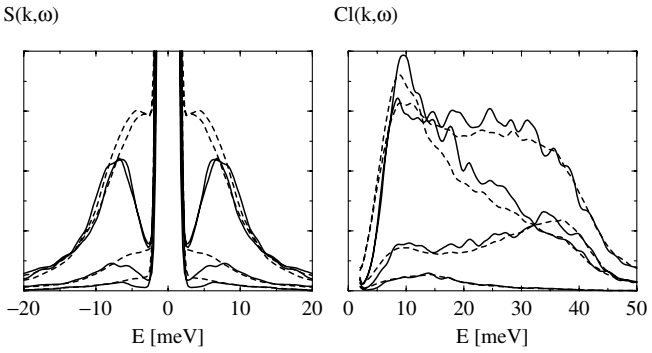

FIG. 6. Coherent dynamical structure factors (left) and corresponding longitudinal spectra (right) of the hydration water from MD simulations of the RNase crystal at 150 K, for the unconstrained system (dashed lines) and the system with the protein atoms fixed (solid lines). From bottom to top: spectra for $k = 0.5$, 1.5, 2.5, and 3.5 Å^{-1}. Note the damping of the boson peak intensity ($\approx$ 3–4 meV) in $S(k, E)$ as the protein motion is hindered, while the 10 meV and $\approx$ 30 meV Brillouin peaks (sound modes) are not affected.

show clearly that the frequencies of the two sound modes (Brillouin peaks), as well as their k dependence, are similar in both the unconstrained and constrained systems. Thus, it is clear that boson peak excitations are distinct from sound modes in protein hydration water.

We have used MD simulations to study the dynamics of single particle and collective density fluctuations of protein hydration water in a protein crystal. We have identified two Brillouin peaks in the coherent longitudinal current spectra, corresponding to modes commonly referred to as ordinary and fast sound in liquid water [8]. We have demonstrated that the boson peak in the single particle spectra of protein hydration water arises exclusively from translational motion. We have perturbed the water dynamics by performing simulations in which the protein backbone atoms were constrained. Comparison of unconstrained and constrained simulations demonstrated that the boson peak excitations are distinct from the TA_1 mode in the incoherent spectra and that the boson peak is present and distinct from the sound modes in the coherent spectra. The latter is consistent with recent experimental observations concerning the connection between the boson peak and sound modes in glassy glycerol and vitreous silica [24,25]. This paper should help further clarify the similarities and differences in the dynamics of liquid and protein hydration water.

This research was supported in part by the National Science Foundation (Grant No. MCB-0078278 to D. J. T.).

*Present address: Equipe de chimie et biochimie théorique, UMR CNRS/UHP 7565, Université Henri Poincaré, 54506 Vandoeuvre-lès-Nancy, France.

[1] C. Mattos, Trends Biochem. Sci. **27**, 203 (2002).
[2] V. P. Denisov and B. Halle, J. Mol. Biol. **245**, 682 (1995); Biochemistry **37**, 9595 (1998); B. Halle, in *Hydration Processes in Biology: Theoretical and Experimental Approaches*, edited by M. C. Bellissent-Funel (IOS Press, Amsterdam, 1999), pp. 233–249.
[3] C. F. Polnaszek and R. G. Bryant, J. Chem. Phys. **81**, 4038 (1984); H. J. B. Steinhoff *et al.*, Biophys. J. **65**, 1486 (1993); G. Otting and K. Wuthrich, J. Am. Chem. Soc. **111**, 1871 (1989); G. Otting, E. Liepinsh, and K. Wuthrich, Science **254**, 974 (1991); G. Otting, Prog. Nucl. Magn. Reson. Spectrosc. **31**, 259 (1997).
[4] M. Settles and W. Doster, Faraday Discuss. **103**, 269 (1996).
[5] A. Paciaroni, A. R. Bizzarri, and S. Cannistraro, Phys. Rev. E **60**, R2476 (1999).
[6] M. Tarek and D. J. Tobias, J. Am. Chem. Soc. **121**, 9740 (1999).
[7] M. Tarek and D. J. Tobias, Biophys. J. **79**, 3330 (2000).
[8] A. Rahman and F. H. Stillinger, Phys. Rev. A **1**, 368 (1974).
[9] P. Bosi, F. Dupré, F. Menzeinger, F. Sachetti, and M. C. Spinelli, Nuovo Cimento Lett. **12**, 436 (1978).
[10] J. Teixeira, M. C. Bellissent-Funel, S. H. Chen, and B. Dorner, Phys. Rev. Lett. **54**, 2681 (1985).
[11] F. Sette *et al.*, Phys. Rev. Lett. **75**, 850 (1995).
[12] G. Ruocco *et al.*, Nature (London) **379**, 521 (1996).
[13] F. Sette *et al.*, Phys. Rev. Lett. **77**, 83 (1996).
[14] A. D. MacKerell, Jr. *et al.*, J. Phys. Chem. B **102**, 3586 (1998).
[15] H. J. C. Berendsen, J. R. Grigera, and T. P. Straatsma, J. Phys. Chem. **91**, 6269 (1987).
[16] G. J. Martyna, D. J. Tobias, and M. L. Klein, J. Chem. Phys. **101**, 4177 (1994).
[17] G. J. Martyna, M. E. Tuckerman, D. J. Tobias, and M. L. Klein, Mol. Phys. **87**, 1117 (1996); M. E. Tuckerman *et al.*, Comput. Phys. Commun. **128**, 333 (2000).
[18] M. Tarek, D. J. Tobias, S. H. Chen, and M. L. Klein, Phys. Rev. Lett. **87**, 238101 (2001).
[19] In the simulation the $\mathbf{k}$ vectors are restricted to have the values $\mathbf{k} = l\mathbf{a}_i^* + m\mathbf{a}_j^* + n\mathbf{a}_k^*$, where l, m, and n are integers and $\mathbf{a}_i^*$, $\mathbf{a}_j^*$, and $\mathbf{a}_k^*$ are the reciprocal lattice vectors. The values of $|\mathbf{k}|$ where chosen between 0.5 and 3.9 Å^{-1} at 0.1 Å^{-1} intervals, and the number of contributing vectors (values of l, n, and m) to each $|\mathbf{k}|$ varied from 60 to 100.
[20] G. Ruocco and F. Sette, J. Phys. Condens. Matter **11**, R259 (1999).
[21] M. Sampoli, G. Ruocco, and F. Sette, Phys. Rev. Lett. **79**, 1678 (1997).
[22] M. Sakamoto, *et al.*, J. Phys. Soc. Jpn. **17**, 370 (1962); A. P. Sokolov, J. Hurst, and D. Quitmann, Phys. Rev. B **51**, 12865 (1995).
[23] M. Tarek and D. J. Tobias, J. Chem. Phys. **115**, 1607 (2001).
[24] C. Masciovecchio, A. Mermet, G. Ruocco, and F. Sette, Phys. Rev. Lett. **85**, 1266 (2000).
[25] O. Pilla *et al.*, Phys. Rev. Lett. **85**, 2136 (2000).